Phase-locked phase-shifting laser diode interferometer with photothermal modulation

Takamasa Suzuki, Xuefeng Zhao, and Osami Sasaki

We propose a phase-shifting interferometer that uses both phase-locked and photothermal modulating techniques. In this interferometer the measurement accuracy is not affected by the intensity modulation that usually appears in current modulation. The surface profile of a diamond-turned aluminum disk was measured; the rms repeatability obtained was $\lambda/460$. © 2001 Optical Society of America

OCIS codes: 120.3180, 120.5060, 140.2020, 120.6660, 120.5050, 140.6810.

1. Introduction

Current or direct modulation in a laser diode (LD) is commonly used in the construction of a variety of interferometers in which no additional phase shifters are required. In LD interferometers it is easy to change the wavelength of the LD and get the desired phase modulation by using triangular,[1,2] rectangular,[3] or sinusoidal[4] injection current. In a phase-shifting interferometry (PSI), for example, one achieves the phase shift by varying the injection current stepwise. Major problems that we have to take into consideration in PSI are the intensity change and control of the phase in the phase shifting. Conventional current modulation affects not only the wavelength but also the intensity of the laser beam, irrespective of modulating wave form. This intensity change has been compensated for electronically[1] or numerically[3] to suppress measurement error in the conventional LD interferometers. The error that is due to the intensity change was also evaluated theoretically.[5] The last-named problem of phase control can be settled with calibrated modulation efficiency[3] or with a computer-controlled injection current.[6]

In this paper we propose a phase-locked, phase-shifting LD interferometer that utilizes photothermal modulation.[7] In our phase-shifting interferometer, the intensity change can be dramatically reduced with this modulating technique, and the phase shift is precisely accomplished with a feedback control that features a phase-locked technique.[8,9] The originality of our technique lies in the fact that the phase lock is achieved not with a current feedback but with an optical feedback. Photothermal modulation of the wavelength of the LD reduces variation of the bias intensity in the fringe images through the entire 2π phase shift. Moreover, external disturbances and the phase-shift error that results from fluctuation of the wavelength are eliminated by means of feedback control. Therefore, both problems that we have cited can be settled in a simple way, and a highly accurate phase-shifting interferometer is achieved with our technique.

In Section 2 we describe the principle of PSI combined with a photothermal modulating technique and with a phase-locked technique. The experimental setup and our results are described in Sections 3 and 4, respectively.

2. Principle

A schematic of the setup is shown in Fig. 1. It consists of three parts: a photothermal modulating system, a feedback-control system, and a fringe analyzing system.

A. Photothermal Modulating System

PSI is a well-established technique. A simple equation for evaluating the phase is[10]

$$\Phi(x, y) = \tan^{-1}\left[\frac{I_2(x, y) - I_4(x, y)}{I_1(x, y) - I_3(x, y)}\right], \qquad (1)$$

The authors are with the Faculty of Engineering, Niigata University, 8050 Ikarashi 2, Niigata 950-2181, Japan. T. Suzuki's e-mail address is takamasa@eng.niigata-u.ac.jp.

Received 25 June 2000; revised manuscript received 2 January 2001.

0003-6935/01/132126-06$15.00/0

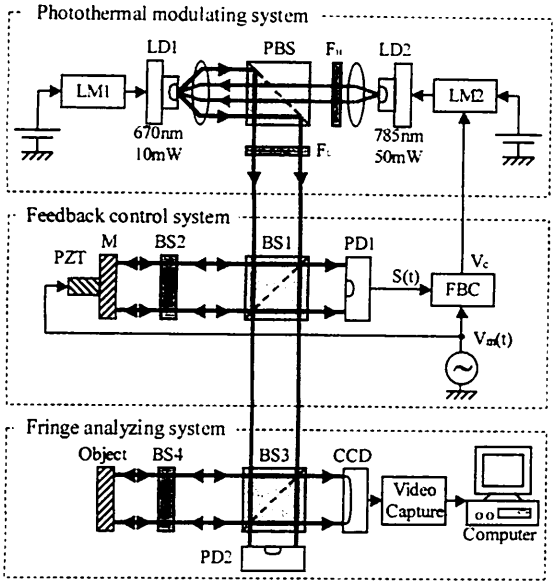

Fig. 1. Experimental setup: Abbreviations are defined in text.

where $\Phi(x, y)$ is the phase to be measured. $I_i(x, y)$ are the intensity distributions in the detected fringes. They can be represented by

$$I_i(x,y) = I_0(x,y)\left\{1 + V(x,y)\cos\left[\Phi(x, y) + (i - 1)\frac{\pi}{2}\right]\right\} \quad (i = 1\text{–}4), \tag{2}$$

where $I_0(x, y)$ is the bias intensity distribution and $V(x, y)$ is the visibility in the interference pattern. To get an accurate measurement result one must keep $I_0(x, y)$ constant through the entire 2π phase shift. In other LD interferometers the phase steps $(i - 1)\pi/2$ were introduced by use of current modulation. Unfortunately, the injection current affects not only the wavelength but also the bias intensity of the interference pattern, which in turn affects the measurement accuracy. In our experiment we applied photothermal modulation by employing two LD's, as shown in Fig. 1, to solve this problem. The process of photothermal modulation was described in Ref. 7. Here we summarize it briefly. It is well known that the wavelength and the output power of the LD vary relative to the injection current as well as to the temperature. In photothermal modulation, source laser diode LD1 is injected only with dc bias current. The intensity-modulated laser beam emitted from heating laser diode LD2 is fed into LD1 through the exit pupil and heats the laser chip in LD1. The temperature change greatly influences the wavelength of the LD but only slightly affects the output power of the LD because the threshold current of the LD increases with temperature.[11] In our system, LD1 is driven only by dc current; the intensity does not change with respect to the injection current. Therefore we can obtain an accurate phase shift with a small intensity change.

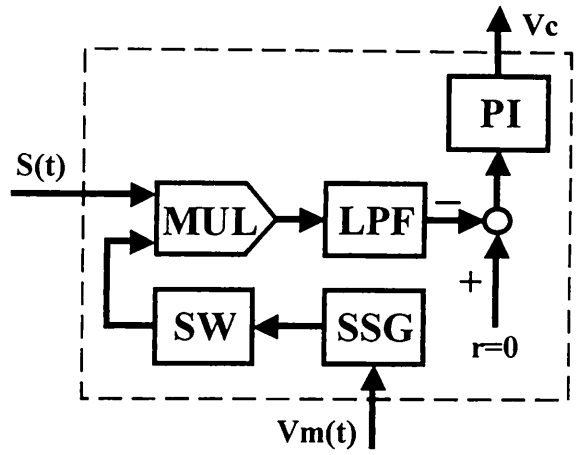

Fig. 2. Block diagram of the feedback controller. MUL, multiplier; PI, proportional-integral controller; other abbreviations are defined in text.

B. Feedback-Control System

In the feedback-control system a Fizeau interferometer with an optical path difference L is used to generate a feedback signal. Mirror M, attached to a piezoelectric transducer (PZT), is driven by a sinusoidal modulating signal:

$$V_m(t) = r\cos(\omega_c t + \theta). \tag{3}$$

If photothermal modulation is employed simultaneously, the temporal change in the interference signals detected by a photodetector (PD1) is given by[12]

$$S(t) = S_1 + S_0\cos[z\cos(\omega_c t + \theta) + \alpha_{FBC}], \tag{4}$$

where

$$z = 4\pi r/\lambda_1 \tag{5}$$

is the modulating depth and

$$\alpha_{FBC} = \frac{4\pi L}{\lambda_1} - \frac{4\pi L}{\lambda_1^2}\beta\Delta I \tag{6}$$

is the phase to be controlled. $S_1, S_0, \lambda_1, \beta$, and ΔI are the dc component, the amplitude of the ac component, the nominal wavelength of LD1 determined by the dc bias current, the modulating efficiency in the photothermal modulation, and the injection current for LD2, respectively.

The synchronous detection that was described in Ref. 12 is now used in the feedback controller of the present measurement to generate feedback signals. A block diagram of the feedback controller is shown in Fig. 2. SSG is the synchronous signal generator, in which four synchronous signals,

$$V_{s1} = -A_{s1}\cos(\omega_c t + \theta), \tag{7}$$

$$V_{s2} = A_{s2}\cos(2\omega_c t + 2\theta), \tag{8}$$

$$V_{s3} = A_{s3}\cos(\omega_c t + \theta), \tag{9}$$

$$V_{s4} = -A_{s4}\cos(2\omega_c t + 2\theta), \tag{10}$$

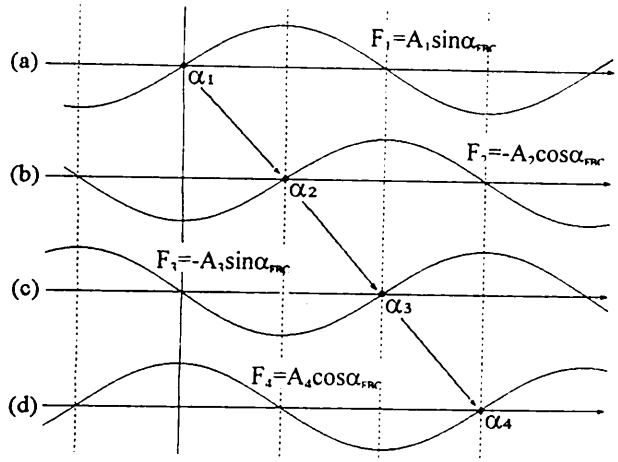

Fig. 3. Phase shifting by the transition of feedback signals F_i.

are generated by the piezoelectric transducer driving signal $V_m(t)$ [Eq. (3)]. They are fed to the multiplier through a switch (SW), which selects one of four signals shown above. Interference signal $S(t)$ given by Eq. (4) is rewritten as

$$S(t) = S_1 + S_0 \cos \alpha_{FBC}[J_0(z) - 2J_2(z)\cos(2\omega_c t + 2\theta) + \ldots] - S_0 \sin \alpha_{FBC}[2J_1(z)\cos(\omega_c t + \theta) - 2J_3(z)\cos(3\omega_c t + 3\theta) + \ldots], \quad (11)$$

where $J_n(z)$ is the nth-order Bessel function. Multiplying $S(t)$ by V_{si} (i = 1–4) and passing it through the low-pass filter (LPF), we obtain four feedback signals[13]:

$$F_i = A_i \sin\left[\alpha_{FBC} - (i-1)\frac{\pi}{2}\right] \qquad (i = 1\text{–}4). \quad (12)$$

When the feedback control is implemented to achieve the condition that $F_i = 0$, phase α_{FBC} is locked at the stable phase $(i - 1)\pi/2$, which is the interaction between the ground level and the region of positive inclination on the feedback signal. Then the phase of the interference signal detected by PD1 is locked. If we use this phase-locked technique with feedback signal F_1, for instance, α_{FBC} is locked at $\alpha_1 = 0$ rad. At the same time, the external disturbances are also eliminated.[12] The entire phase-shifting process in our interferometer is shown in Fig. 3. We implement the phase-locked technique four times by sequentially changing the feedback signal. Consequently, we can achieve a phase shift of $\pi/2$ accurately in PSI.

Because the LD's wavelength varies with temperature, most LD interferometers need temperature control to prevent this fluctuation. This change, however, is quite small compared with a nominal wavelength, and the phase is exactly controlled to the desired value by the phase-locked technique. Therefore, no temperature control is integrated into our system.

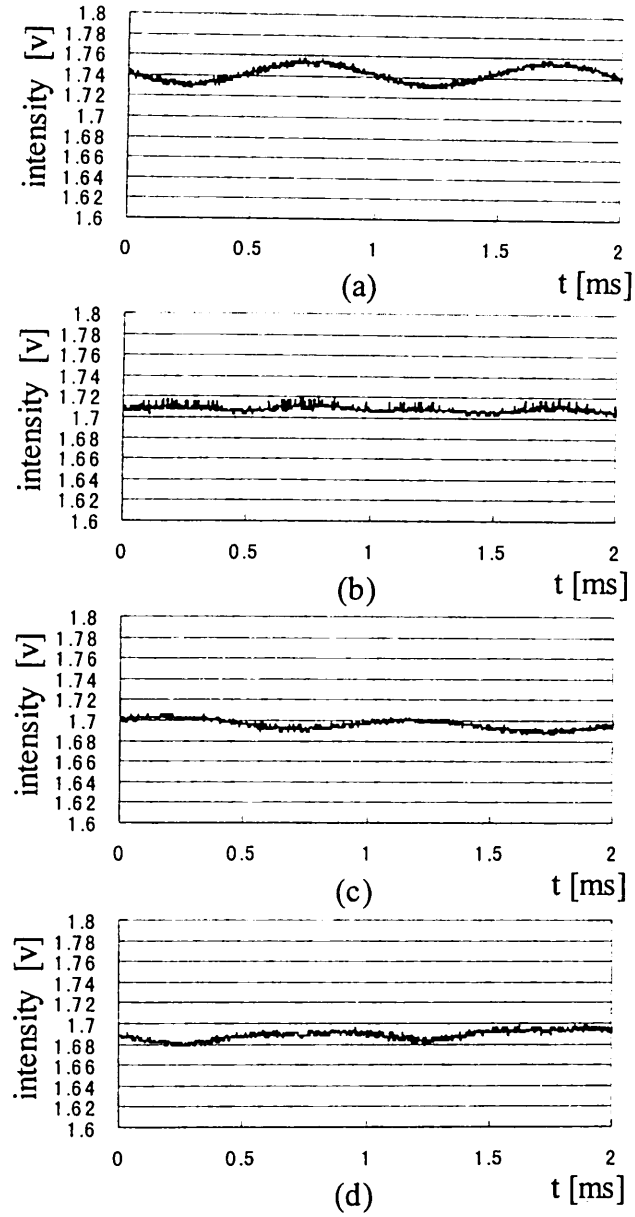

Fig. 4. Intensity changes caused by current modulation. The amount of phase shift is (a) $\alpha_1 = 0$, (b) $\alpha_2 = \pi/2$, (c) $\alpha_3 = \pi$, and (d) $\alpha_4 = 3\pi/2$.

C. Fringe Analyzing System

In the fringe analyzing system we used a Fizeau-type interferometer as we did in the feedback-control system. The amount of the phase shift is proportional to both the variation of the wavelength and the optical path difference (OPD) of the interferometer. As we assume these two Fizeau-type interferometers have same OPD L, the interference fringe captured by the CCD camera contains the same phase shift that is made in the feedback-control system.

D. Measurement Error

We examined the error caused by the difference between the OPD's in the feedback-control system and in the fringe analyzing system. When we adjust the

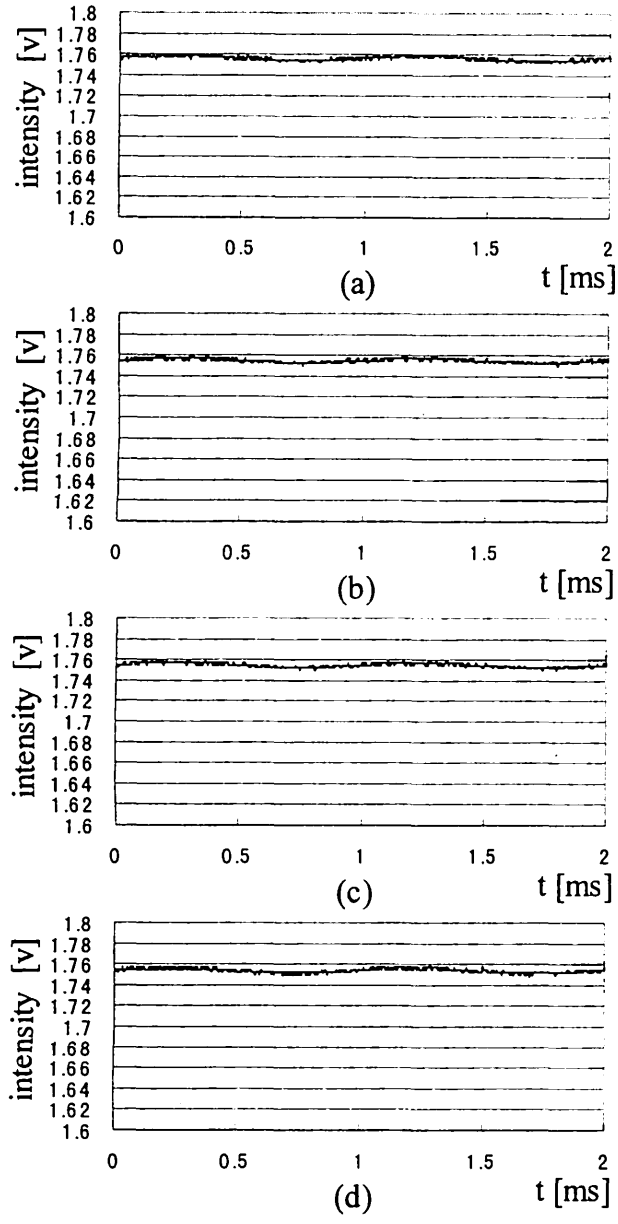

Fig. 5. Intensity change with photothermal modulation. The amount of phase shift is (a) $\alpha_1 = 0$, (b) $\alpha_2 = \pi/2$, (c) $\alpha_3 = \pi$, and (d) $\alpha_4 = 3\pi/2$.

OPD's of the two Fizeau interferometers, there is a small difference ΔL between them that arises because of the difficulty of mechanical adjustment. Therefore a small deviation related to ΔL occurs as[10]

$$\Delta\Phi(x, y) = \frac{\partial\Phi(x, y)}{\partial L}\Delta L = \frac{4\pi}{\lambda_1}\Delta L - \frac{4\pi}{\lambda_1^2}\beta\Delta I\Delta L. \quad (13)$$

Inasmuch as the first term, $4\pi\Delta L/\lambda_1$, has a constant value and can be discarded, the phase-shifting error caused by ΔL is given by the second term in Eq. (13).

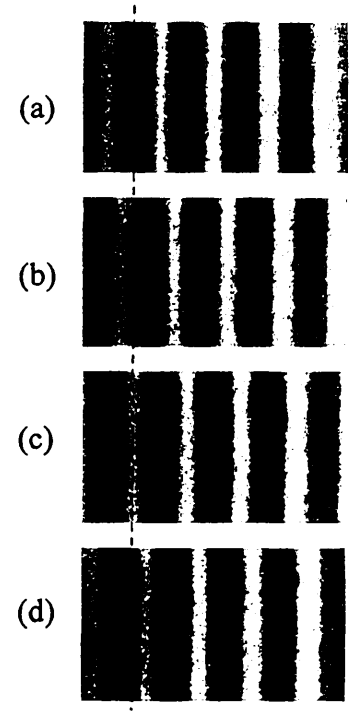

Fig. 6. Fringe images observed with the phase shift.

3. Experimental Setup

The experimental setup is shown in Fig. 1. The maximum output power and the nominal wavelength are $P_1 = 10$ mW and $\lambda_1 = 670$ nm, respectively, for LD1 and $P_2 = 50$ mW and $\lambda_2 = 785$ nm for LD2. The polarizations of the LD's are perpendicular to each other to prevent interference between LD1 and LD2.

The laser beam radiated from LD1 is mostly reflected by the polarizing beam splitter (PBS) and fed into another optical system, whereas the portion that passes through the PBS is reflected on the cover glass of LD2 and returned to LD1. This returning light induces instability in LD1. We used optical high-pass filter F_H, whose cut-off wavelength is 720 nm, to prevent this instability. A part of the heating laser beam is also reflected on the cover glass of LD1. The beam goes to both the feedback-control system and the fringe analyzing system. This useless light, however, is removed by optical low-pass filter F_L, whose cut-off wavelength is 700 nm. All these optical parts, LD1, LD2, F_H, F_L, and PBS, are arranged close together on the same bench to prevent misalignment caused by mechanical vibration. Modulation efficiency[7] β was 1.87×10^{-4} nm/mA in this photothermal modulating system.

In the feedback-control system, M vibrates with the sinusoidal signal [Eq. (3)]. The vibration frequency is 1 kHz. The same sinusoidal signal is also used to generate a feedback signal. The OPD of the interferometers is 60 mm. In this system the control signal generated by the FBC is injected into LD2 to shift the wavelength of LD1. The cut-off frequency of LPF shown in Fig. 2 is 100 Hz. In the fringe analyzing system we used a CCD camera whose pixel

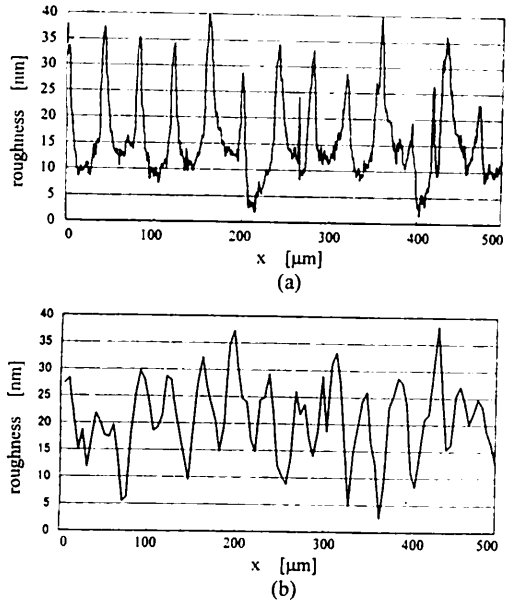

Fig. 7. Two-dimensional surface profiles of a diamond-turned aluminum disk measured with (a) a Talystep profilometer and (b) our system.

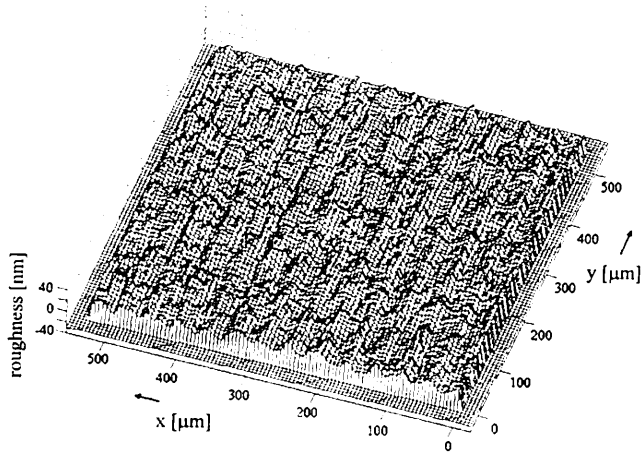

Fig. 8. Three-dimensional surface profile of a diamond-turned aluminum disk measured with our system.

number and shutter speed were 768 × 494 and 1/10000 s, respectively.

An x-axis stage whose resolution ΔL of 10 μm is used, so optical path difference L is set to equal to that in the feedback-control system. We first roughly adjusted the OPD with an ordinary ruler and measured a two-dimensional surface profile of the object. If the OPD's between the feedback-control system and the fringe analyzing system are not exactly the same, the measured profile will contain nonlinearity. Next we adjusted the OPD by using the x-axis stage and measured the profile repeatedly until the nonlinearity was removed.

The phase-shifting error in Eq. (13) is estimated as 5.2×10^{-4} rad because λ_0, ΔL, β, and the maximum value of ΔI are 670 nm, 10 μm, 1.87×10^{-4} nm/mA, and 10 mA, respectively, in our experiment. The error is small, and we can neglect it.

4. Results

We measured the intensity change of the optical source by shifting the phase by using the phase-locked technique. The results shown in Fig. 4 were measured with current modulation. In these figures, both the dc and the ac components of the intensity are obviously changing. The sinusoidal change is caused by leakage of the synchronous signals V_{si} [Eqs. (7)–(10)]. The change in the level of dc components indicates that the bias intensity of the interference pattern varied widely while phase shifting was obtained. The intensity changes measured with the photothermal modulation were dramatically reduced, as shown in Fig. 5. The level of dc components does not change much in Fig. 5.

We used a flat mirror as an object and measured four fringes by sequentially shifting the phase by $\pi/2$. Results are shown in Fig. 6. Because the external disturbances were eliminated by the feedback control, clear fringes were detected. The dashed lines in Fig. 6 are reference lines with which the phase shifts can be checked. The amount of each phase shift was adjusted $\pi/2$ automatically by the phase-lock control. It was confirmed that an exact phase shift was realized and that the bias intensity was not affected by the phase shift.

The surface profile of a diamond-turned aluminum disk whose cutting pitch was ~40 nm was measured. Two-dimensional results measured with a Talystep profilometer and with our system are shown in Fig. 7. They show a periodic structure determined by the cutting pitch. Measured points in Figs. 7(a) and 7(b) are different; however, the cutting pitch and the roughness of these results agree with each other. Figure 8 shows three-dimensional results obtained with our measurement system. The period and roughness agree well with those measured with the Talystep profilometer. We measured the same disk several times at intervals of a few minutes. The repeatability in the measurements was λ/460 rms.

5. Conclusions

A phase-shifting laser diode interferometer that uses both phase-locked and photothermal modulating techniques has been described and demonstrated. The former technique enables us to achieve accurate phase shifting and eliminate external disturbances. The bias intensity of the detected fringe pattern did not vary in the phase-shifting process in the latter technique. The measurements of the diamond-turned aluminum disk showed that the proposed interferometer has a measurement repeatability of λ/460 rms.

References

1. K. Tatsuno and Y. Tsunoda, "Diode laser direct modulation heterodyne interferometer," Appl. Opt. **26**, 37–40 (1987).
2. J. Chen, Y. Ishii, and K. Murata, "Heterodyne interferometry

with a frequency-modulated laser diode," Appl. Opt. **27,** 124–128 (1988).
3. Y. Ishii, J. Chen, and K. Murata, "Digital phase-measuring interferometry with a tunable laser diode," Opt. Lett. **12,** 233–235 (1987).
4. T. Suzuki, O. Sasaki, K. Higuchi, and T. Maruyama, "Real-time displacement measurement in sinusoidal phase modulating interferometry," Appl. Opt. **28,** 5270–5274 (1989).
5. P. Hariharan, "Phase-stepping interferometry with laser diodes: effect of changes in laser power with output wavelength," Appl. Opt. **28,** 27–28 (1989).
6. Y. Ishii, "Recent developments in laser-diode interferometry," Opt. Laser Eng. **14,** 293–309 (1991).
7. T. Suzuki, M. Matsuda, O. Sasaki, and T. Maruyama, "Laser-diode interferometer with a photothermal modulation," Appl. Opt. **38,** 7069–7075 (1999).
8. T. Suzuki, O. Sasaki, and T. Maruyama, "Phase locked laser diode interferometer for surface profile measurement," Appl. Opt. **28,** 4407–4410 (1989).
9. T. Suzuki, T. Muto, O. Sasaki, and T. Maruyama, "Wavelength-multiplexed phase locked laser diode interferometer using a phase-shifting technique," Appl. Opt. **36,** 6196–6201 (1997).
10. J. Schwider, R. Burow, K.-E. Elssner, J. Grzanna, R. Spolaczyk, and K. Merkel, "Digital wave-front measuring interferometry: some systematic error sources," Appl. Opt. **22,** 3421–3432 (1983).
11. P. Blood, E. D. Fletcher, K. Woodbridge, K. C. Heasman, and A. R. Adams, "Influence of the barriers on the temperature dependence of threshold current in GaAs/AlGaAs quantum well lasers," IEEE J. Quantum Electron. **25,** 1459–1468 (1989).
12. O. Sasaki, K. Takahashi, and T. Suzuki, "Sinusoidal phase modulating laser diode interferometer with a feedback control system to eliminate external disturbance," Opt. Eng. **29,** 1511–1515 (1991).
13. T. Suzuki, O. Sasaki, S. Takayama, and T. Maruyama, "Real-time displacement measurement using synchronous detection in a sinusoidal phase modulating interferometer," Opt. Eng. **32,** 1033–1037 (1993).